# Avalanchelike bursts in global gyrokinetic simulations

B. F. McMillan,[1] S. Jolliet,[1] T. M. Tran,[1] L. Villard,[1] A. Bottino,[2] and P. Angelino[3]
[1]*Centre de Recherches en Physique des Plasmas, Association Euratom-Confédération Suisse, Ecole Polytechnique Fédérale de Lausanne, PPB, 1015 Lausanne, Switzerland*
[2]*IPP-EURATOM Association, Max Planck Institut fur Plasmaphysik, Garching, Germany*
[3]*Association Euratom-CEA, CEA/DSM/DRFC Cadarache, France*

(Received 6 November 2008; accepted 15 January 2009; published online 25 February 2009)

Highly variable flux surface averaged heat fluxes are resolved in gyrokinetic simulations of ion temperature gradient (ITG) turbulence, even in large systems. Radially propagating fronts or *avalanches* are also seen. Their propagation lengths in gyroradii and relative amplitude remain constant as simulation size is increased, so the avalanches appear to result from local dynamics, rather than global relaxation events. For the Cyclone [Dimits *et al.*, Phys. Plasmas **7**, 969 (2000)] case, the avalanche propagation direction is found to depend on the sign of the shearing rate. A mechanism for avalanche propagation based on the advection of turbulence tilted by the shear flows is proposed: The Cyclone linear ITG dispersion relation explains the propagation direction of tilted vortices. It also explains why there is no such preferred direction in a simulation with reduced magnetic shear. The paper explores several models for these bursts. First, certain types of models based on nonlinear heat diffusion equations are ruled out. A different type of one-dimensional (1D) model, introduced in Benkadda *et al.* [Nucl. Fusion **41**, 995 (2001)], yields much better qualitative and quantitative agreement. However, the 1D model cannot explain the directionality of the bursts, even though it includes the features typically considered important for burst propagation. A symmetry-breaking term is necessary. An additional term is included to reproduce the wave dispersion with respect to radial wavenumber, and this is shown to be sufficient to reproduce the favored direction for burst propagation. © *2009 American Institute of Physics*.
[DOI: 10.1063/1.3079076]

## I. INTRODUCTION

Global gyrokinetic simulations of tokamaks (with Cyclone[1] parameters) using the ORB5 code[2] show propagating structures in plots of heat flux versus radius and time. Even though bursts have also been seen in other fluid[3] and gyrokinetic[4] simulations of tokamaks, these structures are not as well characterized or well understood as the processes governing average flux levels. We would like to understand the burst mechanism because infrequent large bursts, if they can propagate through the edge, might directly damage fusion devices. An additional motivation for the study of bursts is model validation, as experimental diagnostics have extensive capacity to measure time variation.

Recent descriptions[5,6] of avalanches have emphasized global physics of flux driven systems. After initially trying to explain avalanche properties in terms of global profile variation, we later found that a convincing model of the avalanches we see in ion temperature gradient (ITG) turbulence involves only local physics (present in the flux-tube limit): The avalanche propagation length scales with the zonal flow width, and other avalanche properties scale with the local turbulence time and length scales. This distinction between global and local physics was difficult to resolve in small systems $\rho_s/a=\rho^* \gtrsim 1/140$ (where $a$ is the plasma minor radius and $\rho_s=\rho_{ti}T_e/T_i$ for thermal ion gyroradius $\rho_{ti}$ and electron and ion temperatures $T_e$ and $T_i$) because of the lack of a clear separation between global and local length scales: Such small systems are only a few times the size of typical wavelengths of turbulence ($\sim 30\rho_s$ for Cyclone parameters) or the radial wavelengths of zonal flows. In systems with $\rho^* \lesssim 1/280$ the separation between the burst and global scales becomes obvious: We examine scaling of burst properties with $\rho^*$.[1]

Because the dynamics of the bursts appear to be strongly interrelated with those of the zonal flows, we wish to have detailed information about the effect of sheared flows on turbulence. One such diagnostic is the local tilting direction of vortices which have been sheared by the local shear flows. We also design a diagnostic to measure the radial propagation direction of heat flux structures, allowing a quantitative exploration of the relationship between shear flows and avalanche propagation direction.

We suggest a model for the burst propagation based on the radial group velocity of tilted turbulence which is consistent with the measurements of the tilted turbulence and the inward and outward propagating bursts. The radial group velocity arises because of the dispersion of the real frequency of ITG modes with respect to radial wavenumber. In order to test this mechanism, we consider a configuration with much lower shear where the turbulence is slablike and the dispersion with respect to radial wavenumber is weaker.

After characterization of the features seen in the simulations, we move on to lower dimensional models of the avalanche process. We explain why the models based on nonlinear heat equations cannot adequately describe the bursts in the ITG results, and how a one-dimensional (1D) model,

 

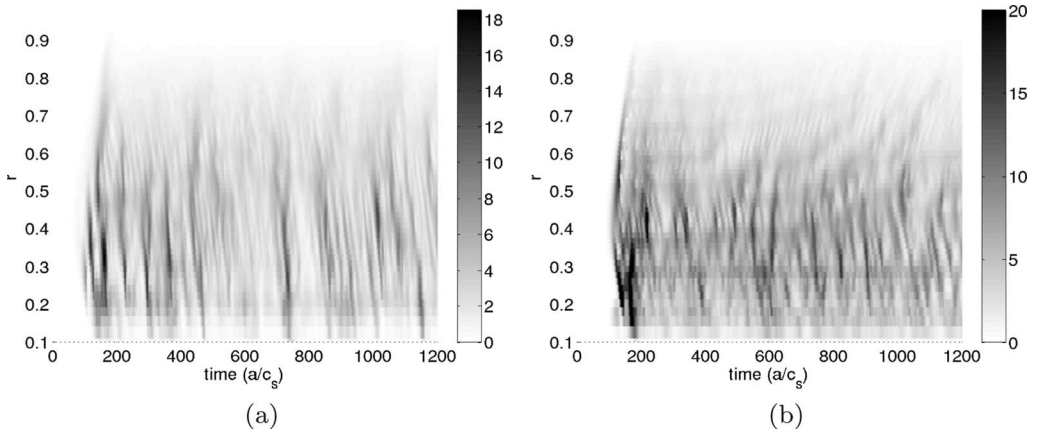


FIG. 1. Heat flux vs $r$ and time in a simulation with $\rho^*=1/140$ (a) and $\rho^*=1/280$ (b) in units of $mn_0\rho^{*2}v_{ti}^3$ ($mn_0$ is the ion mass density at midradius).

partially explored elsewhere,[6] allows significant insight into the underlying burst physics.

## II. RESULTS

Three simulations of collisionless electrostatic ITG turbulence with adiabatic electrons were performed for $\rho^*=\rho_s/a=1/140$, 1/280, and 1/560; the saturated phase was $1500a/c_s$ long (the sound speed $c_s=v_{ti}T_e/T_i$) for the two smaller simulations, and $750a/c_s$ long for the largest simulation, allowing many bursts to be resolved. Temperature gradients are controlled with local heating, which, in the absence of turbulence, ensures that the temperature profile relaxes back to the initial profile with a rate $\gamma_H$. $\gamma_H$ scales with the gyro-Bohm confinement time for the two smaller simulations in order to retain slow variations in the global temperature profile (for the larger simulation we wished to constrain the temperature gradient more tightly for a scaling exercise which will be described in later work); $\gamma_H$ are $0.0127c_s/a$, $3.2\times10^{-3}c_s/a$, and $0.0127c_s/a$ for the small, medium, and large simulations, respectively.

The flux and zonal flow plots (Figs. 1 and 2) versus time and normalized minor radius $r$ of the two smaller simulations are qualitatively quite different to each other: In the $\rho^*=1/140$ simulation, global scale zonal flows develop and flux events are correlated across most of the minor radius, whereas in the medium simulation ($\rho^*=1/280$), the global scale flows are less evident and large flux events propagate over a smaller fraction of the minor radius. Slow global zonal flow profile evolution persists in these simulations,[7] which would possibly reach a quasisteady state over longer timespans (in physical tokamaks this steady state is expected to be collisionality dependent): The simulations test how bursts propagate given a certain (typical) zonal flow profile, rather than making a prediction about the steady state flows. The avalanches' propagation speed does not appear to depend strongly on their amplitude; large and small avalanches run parallel to each other. In the $\rho^*=1/140$ simulation, inward propagating features dominate, but the larger simulation shows a mixture of inward and outward propagating features.

The two-dimensional (radial and temporal) autocorrelation of the time-varying component of the late-time flux (in the window $0.3<r<0.8$) of the $\rho^*=1/140$ simulation is plotted in Fig. 3(a). The correlation magnitude is $<0.1$ beyond time lags $\delta t$ of $50(a/c_s)$. The substantial leftward movement of the maximum correlation point at large $\delta t$ indicates inward propagating structures. At $\delta t=27(a/c_s)$, the maximum correlation is 0.2, with a radial displacement $\delta r=-0.17$, giving a structure velocity of $\sim-0.9\rho^*c_s$, of the same order as typical $E\times B$ velocities. These figures are rela-

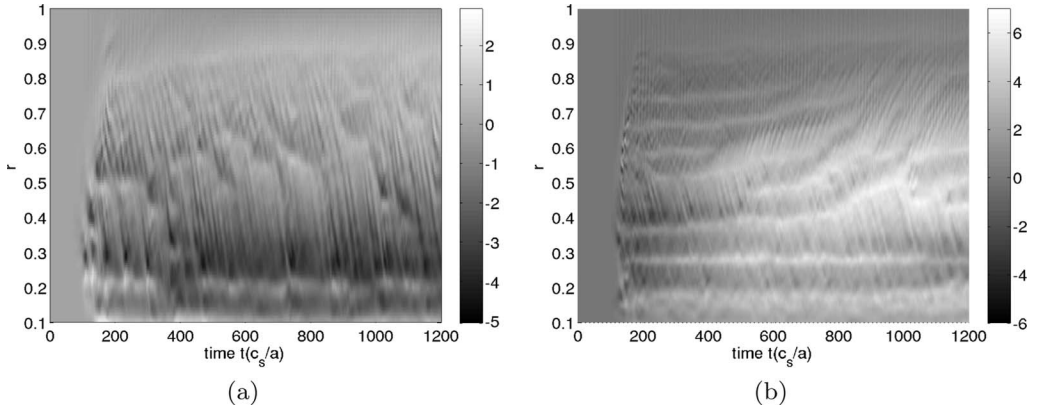


FIG. 2. First radial derivative of zonal potential for (a) the $\rho^*=1/140$ simulation and (b) the $\rho^*=1/280$ simulation (arbitrary units).

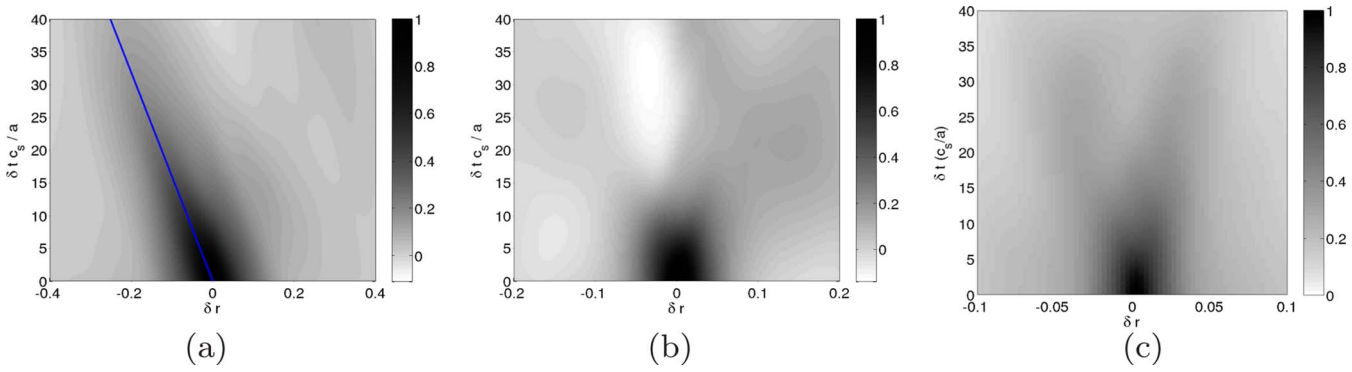


FIG. 3. (Color online) Autocorrelation of time-varying component of the flux vs spatial and temporal offsets, (a) $\rho^*=1/140$ (with a line indicating the structure direction), (b) $\rho^*=1/280$, and (c) $\rho^*=1/560$.

tively robust between different simulations with modified initial conditions, but the measured structure velocity depends of the choice of radial window. After hand-fitting lines onto the burst structures, we found that bursts propagate faster near the axis: at $r=0.49$, $v=-1.17\rho^* c_s$, and at $r=0.78$, $v=-0.40\rho^* c_s$. For the $\rho^*=1/280$ simulation, the autocorrelation analysis ineffective as a means of measuring burst velocity, as both outward and inward propagating bursts are present at the same time (the analysis of Ref. 8 was insufficiently cautious). By hand-fitting lines on the flux plots at $r=0.36$, 0.45, 0.68, and 0.82, absolute structure velocities were measured as 1.2, 0.90, 0.68, and $0.48\rho^* c_s$, respectively. At $\delta t=0$, the full widths at half maximum of the autocorrelation are $\delta r \sim 0.2$, 0.1, and 0.05 for the small, medium, and large simulations, respectively, so that flux correlation lengths are constant in units of gyroradius.

Figure 4 shows the heat flux distributions for $r \in [0.43, 0.56]$ (other curves will be explained later). The burstiness of the flux trace is evident in the long tail of the histogram toward high fluxes: Very large events are much more common than for a normally distributed quantity with the same mean and variance. It is difficult, however, to identify the functional form of the tail because the range of fluxes is relatively small, and a wide class of functions provide an adequate fit.

These propagating bursty features are also seen in the zonal radial electric field (Fig. 2); these bursts are strongly correlated with the bursts of flux. In addition, vertically aligned structures associated with geodesic acoustic modes (GAMs) can be seen toward the plasma edge $s>0.6$, but because these are at higher frequencies than the bursts we are interested in, and do not lead to significant shear flows (GAMs are not evident in Fig. 5), it appears that the GAMs do not play a role in burst dynamics. Apart from the bursts and the GAMs, there is a low-frequency component in the shearing rate plot which is associated with the zonal flows. The rapid fluctuations of the shearing rate are similar in amplitude to the zonal flow shear, so that the net shear drops to around zero during a burst: This suggests that burst driven shear could have a significant backreaction on the bursts themselves. The role of zone boundaries in the dynamics of the bursts is evident in Fig. 2(b), where, in the outer region $r \in [0.4, 0.85]$, the zone boundaries separate inward from outward propagating behavior and also act as "barriers" for

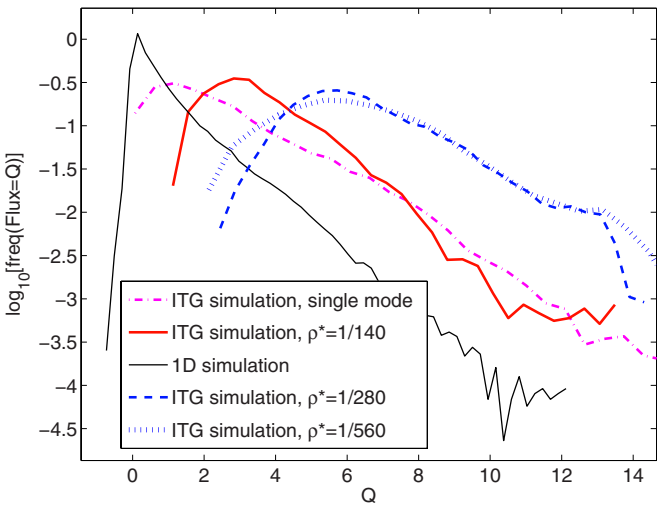


FIG. 4. (Color online) Distribution of the heat flux on the radial range $r \in [0.43, 0.56]$. For the ITG simulations the flux is in units of $mn_0\rho^{*2}v_{ti}^3$.

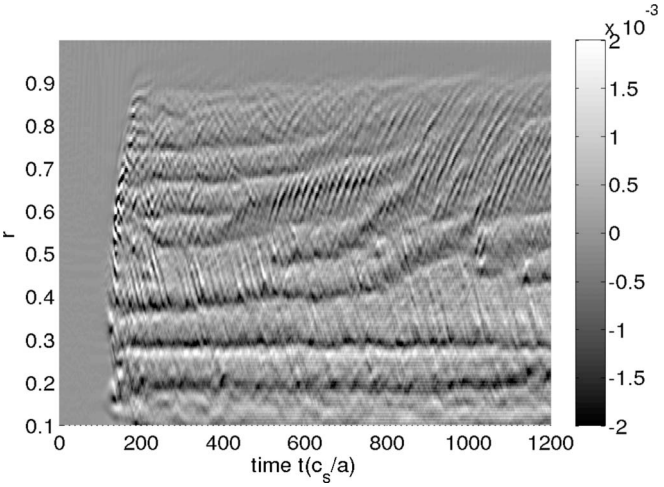


FIG. 5. (a) Second radial derivative of zonal potential for the $\rho^*=1/280$ simulation. Bright regions indicate positive shear and dark regions negative shear (arbitrary units).

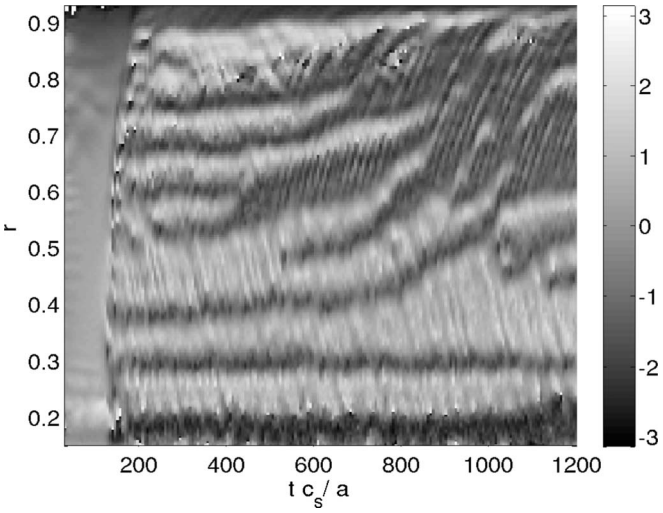


FIG. 6. Tilt angle (radians) of turbulent eddies as a function of time and radius in the Cyclone simulation with $\rho^*=1/280$.

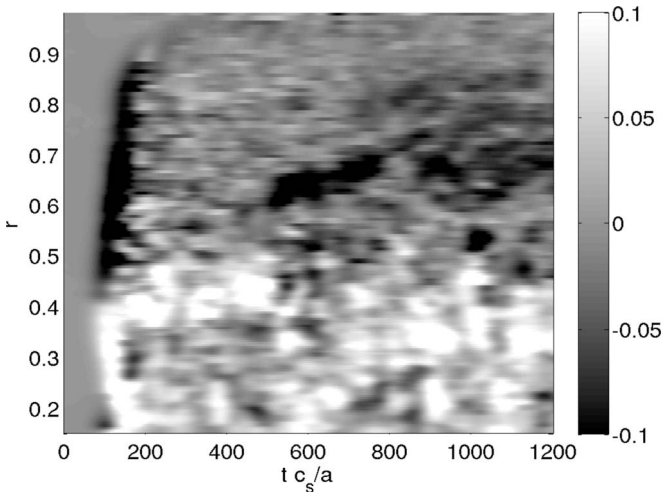


FIG. 7. Propagation direction of bursts as a function of time and radius in the Cyclone simulation with $\rho^*=1/280$: positive values (white) indicate inward propagation; negative values (black) outward propagation.

the bursts, so that their propagation lengths are typically one zone width. Transient simulations show the same association between avalanche direction and the sign of flow shear.

Another property correlated with the shearing rate is the overall tilt of the sheared turbulence, which we quantify by finding average direction of $\nabla\Phi$ on the outboard midplane. Because plane waves have regions with $\nabla\Phi \propto \pm \mathbf{k}$, we need a measure insensitive to the sign of the vector, dependent only on the angle modulo $\pi$: We are interested in the *director* field $\overleftrightarrow{k}$ rather than the vector field $\vec{k}$.[9] One way to define such a measure is to consider the normalized toroidal average $\langle \bar{K} \rangle = \langle K \rangle / |\langle K \rangle|$ of the complex quantity $K=(d\Phi/dr+id\Phi/d\zeta)^2$, which is $-1$ for radially aligned streamers and 1 for striations aligned with the flux surfaces; for structures tilted at $\pi/2$ this quantity is $-i$ or $i$ depending on the direction of the tilt. This analysis is based on techniques used in pattern analysis[9] to recover the local wavevector. A plot of the complex phase of $K$ (in radians) versus radius and time is displayed in Fig. 6 for the $\rho^*=1/280$ simulation. The average tilt of the turbulence (which is quite large, as the turbulence is strongly sheared) correlates quite closely to the local shearing rate: Positive shearing rates are associated with positive average tilts and vice versa.

Our analysis of burst propagation direction is similar to the vortex tilting diagnostic: Given the flux $F(r,t)$, we find the quantity $P(r,t)=\mathrm{Im}[(dF/dr+idF/dt)^2]$ which measures the dominant direction of diagonally aligned structures. Spatial locations with positive $P>0$ correspond to bursts propagating to smaller $x$ with increasing time and vice versa for $P<0$. We plot the smoothed version of this quantity in Fig. 7 (smoothed using a Gaussian with a full width of $100a/c_s$). This quantity agrees with the visual impression of domination of inward propagation in some regions and outward propagation in other regions. At the start of the simulation we see inward and outward propagations as the turbulent region spreads from midradius to the axis and edge of the tokamak. Later on, we see a clearly inward propagating zone from $r\in[0.4,0.5]$, and after $t=500$, an outward propagation region at $r\sim 0.7$. A large proportion of the time and spatial extent is dominated neither by inward nor outward propagating features, consistent with a visual inspection of the flux plots. Smaller shear features do not clearly correlate with a preferred burst direction: It appears that the shear zones must be relatively wide to set up a dominant avalanche direction. The spatially and temporally averaged correlation between the shearing rate $S$ (smoothed over $20a/c_s$) and propagation direction measure is defined via $\langle LS \rangle / (\langle L^2 \rangle \langle S^2 \rangle)^{1/2}$; this correlation is fairly sensitive to the choice of time and space region, but reasonable choices give a negative correlation, with values from around $-0.1$ to $-0.3$. For a spatial window $r\in[0.34,0.84]$ and a temporal average running from $t=230a/c_s$ to the end of the simulation, the values are $-0.265$, $-0.140$, and $-0.142$ for the small, medium, and large simulations, respectively. Two other simulations with $\rho^*=1/140$ but different initial conditions and half the number of markers exhibit correlations of $-0.245$ and $-0.298$.

We suggest that avalanche propagation is influenced by the radial propagation of the tilted waves due to linear dispersion. Consider, as a model of a burst, a radially localized ITG wavepacket, with peak initial radial wavenumber around zero. Once the waves in the packet develop a mean tilt due to flow shear (so $\langle k_r \rangle \neq 0$), a quasilinear model would predict a radial propagation of a turbulent wavepacket with velocity $v_r \sim \langle d\omega/dk_r \rangle$, where $\omega$ is the wave frequency. A dispersion relation in $k_r, k_\theta$ for the most unstable mode was determined using a linear flux-tube gyrokinetic simulation (using the GENE code[10] with midradius parameters), giving plane wave solutions $\exp(i\omega t - i\mathbf{k}.\mathbf{x})$ perpendicular to the magnetic field. We assume that the turbulence is dominated by waves with variation along the field line similar to the most linearly unstable modes, so that this dispersion relation captures the most important linear propagation effects. The spectrum is symmetrical with respect to the sign of $k_r$ for this geometry, and is also periodic in $k_r \rightarrow k_r + 2\pi N \hat{s} k_y$, due to the coupling along the field line and the magnetic shear. In the linear spectrum (Fig. 8), the dependence of the frequency on

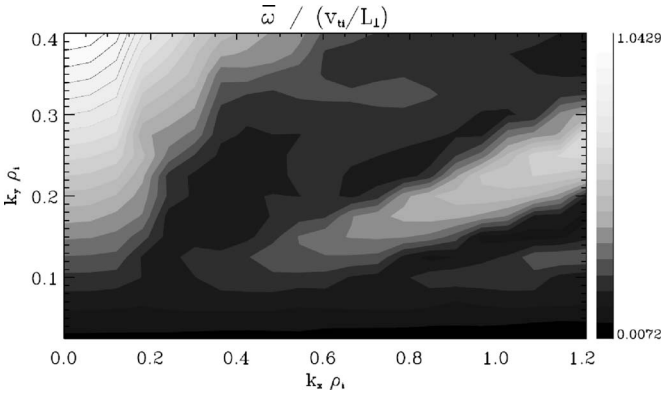


FIG. 8. Frequency vs poloidal and radial wavenumbers for ITG modes in a flux tube with Cyclone parameters.

radial wavenumber is weak for poloidal wavenumbers below $k_y\rho_i=0.1$ ($k_y$ here corresponds roughly to poloidal wavenumber $k_\theta$), but is quite strong for the waves in the range $k_y\rho_i \in [0.15, 0.3]$ where most of the turbulent spectral energy is concentrated. At $k_y\rho_i=0.2$, the dispersion relation can be approximately fitted by $\omega=0.17\rho^* c_s \rho_i^{-1}[1-7.9\rho_i^2 k_r^2]$ for $k_r \lesssim k_y$, so $\partial\omega/\partial k_r=-2.69\rho_i\rho^* c_s k_r$. For tilted turbulence if we typically have $k_r \sim 0.5|k_y|$ the associated absolute velocity is $0.045c_s$. This is larger than the propagation velocity of the bursts by a factor of 4. We also make a prediction about the direction of propagation of the waves: Waves with positive $k_r$ and $k_\theta$ should propagate inward if $\omega$ is positive. In our simulation and coordinate system, the ITG waves propagate in the $\hat{\theta}$ direction and the sign of $\omega$ is positive, as confirmed by examining a plot of potential versus time and poloidal angle. We therefore expect waves with positive $k_r$ and $k_\theta$ to have a group velocity in the negative $r$ direction and propagate inward. For the $\rho^*=1/140$ simulations, the turbulence is predominantly at $k_r/k_\theta>0$ [on the $(R,Z)$ plane of Fig. 9 the $\theta$ direction is anticlockwise and the structures can be seen be slope downward and to the right in the region of intense turbulence on the outboard side], and we would predict inward propagation. The sign of the propagation velocity found in the simulations is therefore in agreement with that predicted from the group velocity propagation mechanism.

As a further exploration of the burst mechanism, we consider a test case with substantially reduced magnetic shear ($q=1.1+0.4s^2$), with slightly reduced temperature gradients, and with a fourfold periodicity imposed on the electric fields (equivalent to simulating a $\pi/2$ wedge of the torus) but with otherwise the same parameters as the $\rho^*=1/140$ simulation. In plots of the zonal flow evolution (Fig. 11), lower levels of long-wavelength zonal flows and fewer structures propagating over a significant radial extent are seen than in the simulations described earlier. Visually, inward and outward propagating features are observed mixed together in the same zone and propagate radially over one or two zones; the direction measure (Fig. 12) does not indicate any regions dominated by either inward or outward going bursts, and there is no significant correlation between the shear flow sign and burst propagation direction. The linear ITG mode frequency (Fig. 10) shows much weaker dispersion in $k_x$ in this reduced

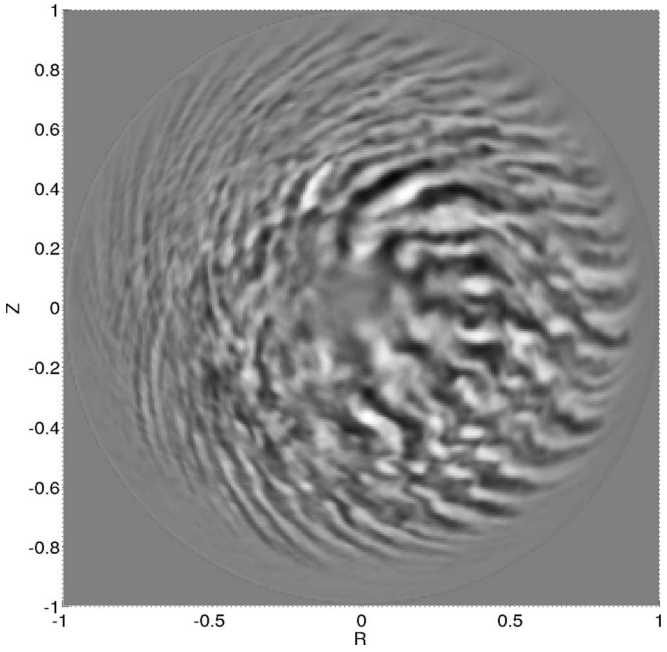


FIG. 9. Nonaxisymmetric component of the electric potential on the poloidal $(R,Z)$ plane for the $\rho^*=1/140$ Cyclone simulation.

shear case, so radial mode dispersion might not be expected to lead to a preferred burst propagation direction; this is consistent with the observed lack of a preferred propagation direction. That bursts propagate at all also tells us that there must be an underlying burst propagation mechanism apart from the linear dispersion of tilted modes.

## III. MODELS BASED ON SELF-ORGANIZED CRITICALITY

Avalanches are a prominent feature of models which exhibit self-organized criticality (SOC).[11] In these models, there is a kind of bistability, which allows an originally stable configuration to be triggered into a state with high levels of flux. In models of grain avalanches, this results from the coefficient of dynamic friction being lower than that of static friction, so the mechanical loads move far from equilibrium as soon as a region begins moving. The ava-

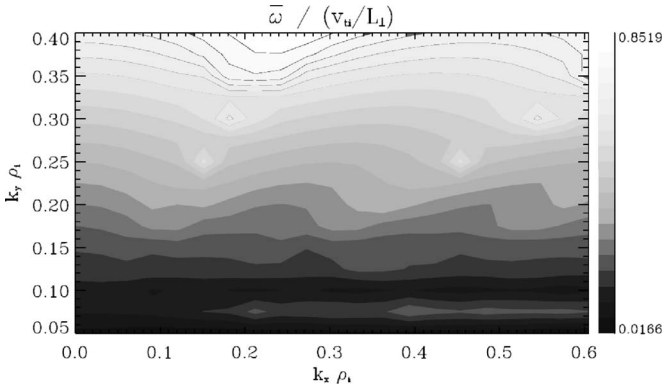


FIG. 10. Frequency vs poloidal and radial wavenumber for ITG modes in a flux tube with Cyclone parameters, but magnetic shear reduced by a factor of 4.

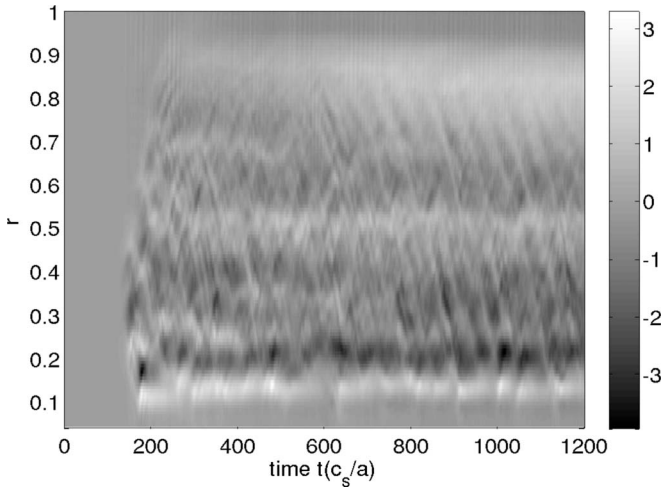


FIG. 11. Radial derivative of zonal potential for a case with a reduced magnetic shear.

lanche is triggered at a particular point when the gradient exceeds some threshold, an instability develops, and the domain of activity spreads.

Discrete sandpile-type models of self-organized criticality are not usually designed to study the dynamics of avalanches. Making the link to simulations with temporal and spatial dynamics usually requires a continuum model. One way of reproducing some features of self-organized criticality in a continuum model is with a quasilinear diffusion[5,12] equation. Such equations can also be physically justified by derivation from fluid models under certain assumptions. A coarse graining over the underlying turbulent structure is performed so that the models are restricted to transport on scales larger than the local length scales. Here, we demonstrate why such models have difficulty explaining the qualitative features of the bursty dynamics of ITG turbulence. In brief, the bursts we see in ITG turbulence do not appear to be similar to those predicted by these quasilinear models. In addition the bursts we see appear to be associated with turbulence-scale physics on short timescales, and on local, rather than global, length scales: Coarse graining cannot easily be justified.

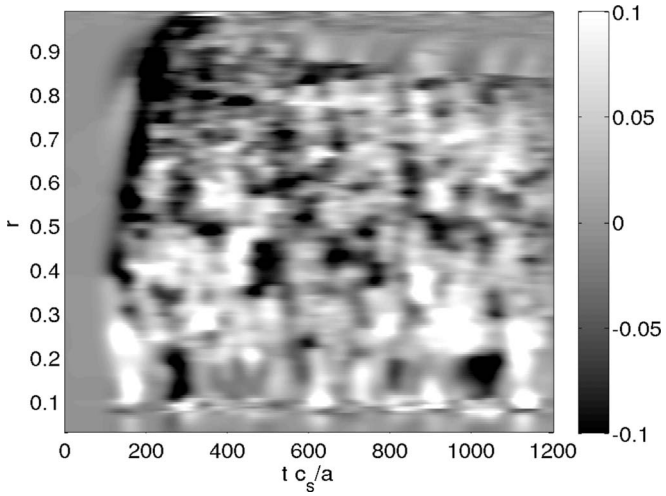


FIG. 12. Measure of direction of burst propagation for a case with a reduced magnetic shear: positive values (white) indicate inward propagation, negative values (black) outward propagation.

As an example, consider the model of Ref. 5, a nonlinear diffusion equation for the evolution of the driving profile, given in their Eqs. (3a) and (3b). Although the linearized form of the equation supports propagating solutions (which are damped on the timescale of the growth rate), it is the nonlinear behavior which is of interest for long term propagating structures. The persistent frontlike solutions derived in Ref. 5 propagate as a traveling wave, with front velocity dependent on amplitude. These solutions do not have the same value at positive and negative $\infty$: The bursts seen in our ITG simulations, on the other hand, are localized. Solving the equations of Ref. 5 with a localized initial inhomogeneity results in a traveling pulse which broadens and reduces in velocity as it propagates, as is typical for a nonlinear diffusion equation.

Burgers' equation is in some sense the canonical form of a nonlinear heat equation; it is also expected from symmetry arguments[12] to be the general form of a coarse-grained continuum model of self-organized criticality. We therefore treat the solutions of Burgers' equation as typical of the kind of avalanches expected in coarse-grained SOC models (including the model of Ref. 5). Burgers' equation can be reduced to a simple linear diffusion equation by an appropriate transform. The solutions to Burgers' equation can then be found directly from the initial conditions.[13] The late-time solutions asymptote toward a class of similarity solutions which in the small/narrow perturbation limit are Gaussian (the equation is equivalent to the standard heat equation in that limit) and in the large/broad limit are triangle shaped. The region of strong flux can propagate to a certain extent to one direction, but broadens and reduces in amplitude and velocity at around the same rate, rather than forming the localized, solitonlike constant-velocity traveling pulses which appear in ITG turbulence. These nonlinear heat equations therefore fail to capture the structure of the bursts. Nor can they explain the origin of these bursts: Ref. 5 had to add an *ad hoc* noise term to obtain nontrivial dynamics, and the predictive power of such a model is somewhat limited, because the burst characteristics tend to depend very strongly on the noise term.

## IV. A LOCAL 1D CONTINUUM MODEL FOR BURSTS

The apparent inadequacy of coarse-grained quasilinear models leads us to consider slightly more complex models which might be able to capture the characteristics of the bursts. The 1D model in Ref. 6 is interesting because it is physically justified based on a derivation from fluid equations and embodies many of the mechanisms underlying ITG turbulence. Below, we explore the qualitative and quantitative features of this model; first, we remove most of the free parameters in the model by rescaling the variables, and we then explain how this model is modified to study collisionless ITG turbulence. The distributions and spectra of the flux in the model are shown to agree well with those in the ITG simulations. Also, the characteristics of the bursts are shown

to agree well with those seen in the simulation. We show, however, that a symmetry of the model makes it incapable of explaining the correlation between the sign of the shearing rate and the burst propagation direction.

Unlike the quasilinear models, the 1D model we examine explicitly solves for the complex wave field as a function of time and radial coordinate, rather than averaging over time or space to produce a model which depends only on the envelope of the turbulent amplitude (but not the phase). Solving for the phase evolution allows the model to capture the dynamics of the interaction between wave tilting and zonal flow generation and the radial breakup of streamers: Including the phase appears to be essential if we wish to capture such dynamics on the inverse growth timescale and on the spatial size of order of the typical radial wavenumber.

As well as flux saturation by zonal flow generation, the dynamics display self-organized avalanchelike bursts for certain parameter choices. This model evolves four 1D fields: a zonal electric potential, a zonal averaged density field, a (complex) wave potential, and a (complex) wave density. The phase of the single mode retained is used to capture the zonal flow coupling: Radial variation in the complex phase (caused by flow shearing) results in damping due to the radial diffusion terms. In the model, phase rotation caused by flow shearing can only be unwound by the turbulence level dropping to zero at some radial position. This is not the case in the full geometry, where a range of toroidal modes are activated (many modes for large devices), so the flux levels may drop to zero at some poloidal positions, but be nonzero when poloidally averaged. We would expect that this 1D model does not give the correct distribution of instantaneous fluxes near zero flux, but might potentially capture the physics at high flux levels if the bursts are radially coherent, and wave phase is important.

We find that the model is bursty where the diffusivity of the density field is sufficiently small. This appears to be a result of the changing the coefficient in the equation for the surface averaged density, rather than that in the equation for the wave potential: Reducing the wave potential diffusivity makes little difference to the dynamics. When this normalized diffusivity parameter is around 1, about half of the flux in the simulation is diffusive, and at transport barriers the temperature gradients increase somewhat, elevating the diffusive flux, to compensate for the turbulent flux becoming very small. With diffusion dominating at these barriers, stable dynamics results. For modeling ITG turbulence the appropriate limit of this model is that in which the diffusive flux becomes small: Typically it is turbulent physics which drives the flux in a tokamak, rather than collisional diffusion. In the limit where the flux due to diffusion vanishes, the gradient must keep increasing at these barriers until a new instability sets in and the turbulence breaks through the barrier.

On the other hand, the viscosity must be retained in the zonal flow equation in order to model the physical zonal flow saturation, and the diffusivity in the wave equations is necessary to model the radial coupling of the waves which limits the radial wavelength of the turbulence (this coupling may in the physical situation be due to wave dispersion). A more complete model would include the secondary instability of zonal flows which occurs above a certain level of flow shear.[14]

Although Ref. 6 includes a spatially varying source and boundaries in its simulation, we consider a simplified periodic model which is analogous to a flux tube with $x$ restricted to the range $x \in [0, L_x]$. We demonstrate that this model still contains the propagating structures and burstiness which are of interest: The model contains avalanches in the absence of explicit sources or imposed spatial inhomogeneity.

We therefore solve the set the equations

$$\partial_t \tilde{n} = -ik\tilde{n}\partial_x \bar{\phi} + ik\tilde{\phi}\partial_x \bar{n} + D\partial_{xx}\tilde{n}, \tag{1}$$

$$\partial_t \tilde{\phi} = -ik\tilde{\phi}\partial_x \bar{\phi} + \frac{ig\tilde{n}}{kn_0} + D\partial_{xx}\tilde{\phi}, \tag{2}$$

$$\partial_t \bar{n} = ik\partial_x(\tilde{n}^*\tilde{\phi} - \tilde{n}\tilde{\phi}^*), \tag{3}$$

$$\partial_t \partial_x \bar{\phi} = ik\partial_x(\tilde{\phi}\partial_x\tilde{\phi}^* - \tilde{\phi}^*\partial_x\tilde{\phi}) + \nu\partial_{xxx}\bar{\phi}. \tag{4}$$

Many of the parameters can be removed from this model by scale transformations: By rescaling the radial coordinate, the time, and the variables $(\tilde{n}, \tilde{\phi}, \bar{n}, \bar{\phi})$ via

$$t \to \pi t = \left(\frac{n_{\mathrm{eq}}}{g n'_{\mathrm{eq}}}\right)^{1/2} t,$$

$$x \to x_0 x = (D\tau)^{1/2} x, \tag{5}$$

$$E \to E_0 E = \frac{1}{\pi k} E,$$

$$\tilde{\phi} \to \tilde{\phi}_0 \tilde{\phi} = \left(\frac{x_0^2 g n'_{\mathrm{eq}}}{k^2 n_{\mathrm{eq}}}\right)^{1/2} \tilde{\phi},$$

$$\tilde{n} \to \tilde{n}_0 \tilde{n} = \frac{k n_{\mathrm{eq}}}{\tau g} \tilde{\phi}_0 \tilde{n}, \tag{6}$$

$$\bar{n} \to \bar{n}_0 \bar{n} = x_0 n'_{\mathrm{eq}} \bar{n},$$

we obtain the set of equations

$$\partial_t \tilde{n} = -i\tilde{n}E + i\tilde{\phi}(\partial_x \bar{n} - 1) + \partial_{xx}\tilde{n}, \tag{7}$$

$$\partial_t \tilde{\phi} = -i\tilde{\phi}E + i\tilde{n} + \partial_{xx}\tilde{\phi}, \tag{8}$$

$$\partial_t \bar{n} = i\partial_x(\tilde{n}^*\tilde{\phi} - \tilde{n}\tilde{\phi}^*), \tag{9}$$

$$\partial_t E = i\partial_x(\tilde{\phi}\partial_x\tilde{\phi}^* - \tilde{\phi}^*\partial_x\tilde{\phi}) + \nu'\partial_{xx}E, \tag{10}$$

where we have taken the background gradient $\partial_x n_0$ to be negative (otherwise the system is stable and uninteresting) and defined $E = \partial_x \bar{\phi}$. The boundary conditions are given by $\tilde{n}(0) = \tilde{n}(L_x)$, $\tilde{\phi}(0) = \tilde{\phi}(L_x)$, $\bar{n}(0) = \bar{n}(L_x)$, and $E(0) = E(L_x)$.

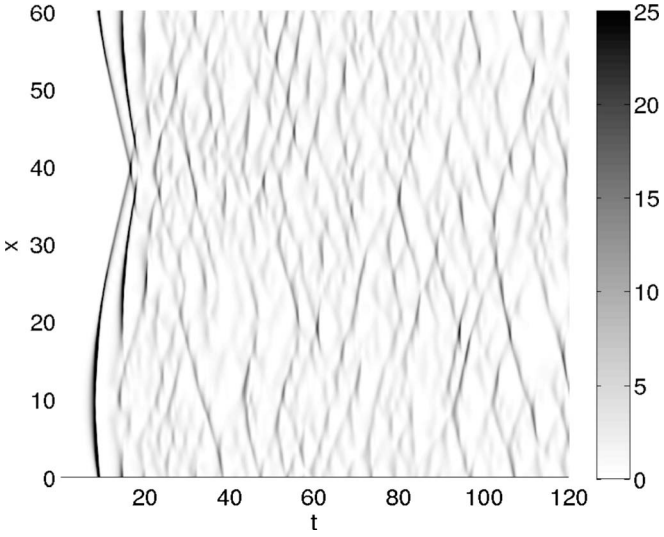


FIG. 13. Flux vs time and radius in the 1D model of ITG turbulence with a background shear flow $E_0'=0.15$.

This set of equations has only one parameter, $\nu'=\nu/D$, which controls the size of the zonal flows relative to the wave diffusion length. This degree of freedom is absent in Ref. 6 because the wave diffusion also acts on the zonal flows (although there was a distinction between viscosity and density diffusion) and arises because we consider the viscosity to be a model for zonal flow saturation, rather than resulting from collisionality. In order for stable zonal flows to be generated, it is necessary that $\nu' \lesssim 8$. The limit $\nu' \ll 1$ results in zonal flows which are narrow compared to the wave diffusion length and which do not show bursts of flux in each zone, but rather a fairly regular oscillatory structure. We could in principle explore this parameter range, but instead, we somewhat arbitrarily choose $\nu=1$ for the moment: This choice will be justified by comparison to the toroidal ITG simulations.

Note that there is no critical gradient in this model: Changing the density gradient simply results in behavior over different length and time scales. The time evolution of this model is very similar to that described in Ref. 6. Complex nonlinear dynamics are seen, including the formation of zonal flows and the propagation of bursts. During some simulations, quite isolated avalanchelike structures are seen in the flux (Fig. 13 is typical).

More controlled numerical experiments are performed to study the nature of the system. First, we impose a background flow shear pattern and examine the propagation of bursts. Consider a background shear flow $xE_0'$, so that the total flow is $E=xE_0'+E_1$. We note that this background flow does not break the up-down symmetry $x\rightarrow -x$ because if $[\tilde{n}(x),\ \tilde{\phi}(x),\ \bar{n}(x),\ xE_0'+E_1(x)]$ is a solution of Eqs. (7)–(10), so is $[\tilde{n}^*(-x),\ -\tilde{\phi}^*(-x),\ -\bar{n}(-x),\ xE_0'-E_1(-x)]$. We therefore expect upward and downward propagating bursts in a zonal flow band with exactly the same statistics (for a randomly chosen ensemble of initial conditions). The simulation domain is periodic, so to maintain translation symmetry in the model with a constant shearing rate we modify the boundary conditions, setting $\tilde{n}(L_x)=\exp(-itL_xE_0')\tilde{n}(0)$ and $\tilde{\phi}(L_x)=\exp(-itL_xE_0')\tilde{\phi}(0)$.

This set of equations is linearly stable for $E_0' \neq 0$ because a finite shearing eventually ensures that the finite time solution is at high radial wavenumber, where it is damped. However, given a small initial perturbation, a very large transient amplification of the perturbation can occur for small values of $E'$: The maximum amplification factor is $\exp(4/3|E_0'|)$. The nonlinear effects can therefore become important even given very small initial perturbations. Nonlinearity allows coupling in $k_r$, so that wave energy may be pumped back into the unstable $k$ range, permitting persistent turbulence. This situation is analogous to that seen in the instability of fluid flow through a pipe:[15] The system exhibits subcritical behavior, a kind of bistability. Also, it is possible to activate time-invariant propagating bursts at high shear levels, given a specific sufficiently large initial perturbation. The large amplitude bursts are able to locally destabilize the system by reducing the local shear flow: The subcritical bursts reduce the shearing rate to approximately zero at the peak position. The presence of a background shear flow is necessary for this bistability to occur: There is a kind of hysteretic relationship between flux and the shearing rate, rather than the usual model of a hysteretic relationship between flux and the background density gradient.

Two burstlike solutions are shown as a function of position and time in Figs. 14(a) and 14(b): They propagate in opposite directions, but are otherwise essentially identical (this is not a surprise in light of the up-down symmetry). The burst solutions cross the simulation domain several times, traveling at an almost constant speed (after an initial transient period) of $2x_0/\tau$, and feature a weak tail with a disordered appearance. The flow shear is $E_0'=1.1$ for the bursts shown. During the transient period the burst amplitude is much lower, but the burst propagation speed is roughly the same as later in the simulation. Figure 15 shows the flux and flow $E$ associated with the burst, using a averaging in a frame moving with burst to remove time variation: The burst carries a net flow with it, and therefore transports momentum.

At more moderate levels of shear $E' \lesssim 0.5$, the system tends to become globally turbulent when activated by a large amplitude perturbation and remain in this state for long times. At $E' \lesssim 0.5$, once sustained turbulence has developed, we have never observed a transition back to a quiescent state. A plot of flux versus radius and time is shown in Fig. 13 for a case with $E'=0.15$ showing a lacework of interacting bursts. All the simulation runs which developed global turbulence exhibited the symmetry of the model in statistical measures like average burst propagation direction.

A histogram of local instantaneous flux levels is shown in Fig. 4. Note that there is a positive probability of seeing small negative flux levels, when the usual phase relation between potential and density fluctuations is reversed (this almost necessarily occurs when either $\tilde{\phi}$ or $\tilde{n}$ have a zero). At large fluxes, there is an exponential decay in the likelihood of seeing a particular level of flux at a given radius. The distribution is highly skewed, with a skewness of $\sim 2.5$. For

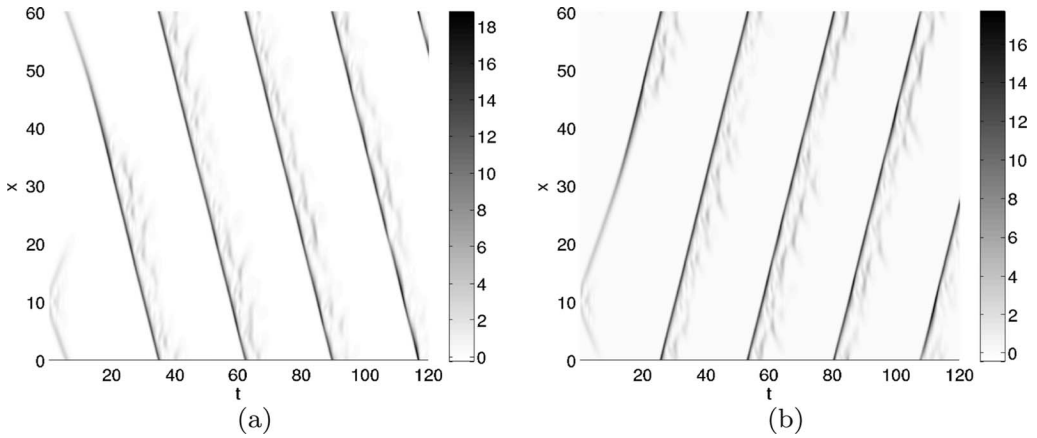


FIG. 14. Flux vs time and radius for a simulation with a solitary propagating structure in the 1D model of ITG turbulence with a background shear flow $E_0'=1.1$. Initial conditions are chosen to give a burst with a (a) positive or (b) negative velocity.

comparison, we plot the normalized flux levels from a simulation with only one toroidal mode. The overall shape is similar, although negative events are much less probable (0.2% versus 6%) in the one-toroidal-mode ITG simulation. The peak of the 1D model's flux distribution is at around zero flux, but that of the single toroidal mode simulation occurs at around $\chi=1$. The difference between these histograms and those of the full ITG simulations is particularly marked at small $\chi$: The multimode simulations have a much smaller probability of being near zero flux, which suggests that the toroidal mode amplitudes are not completely correlated when the flux is low. The exponential decay at large fluxes is, however, similar. Note that an exponential tail is stronger than the tails that would be predicted in a weak turbulence model where the statistics arise as a sum of uncorrelated phases, but still not as strong at seen in many systems with very bursty characteristics which have power-law tails in quantities such as instantaneous flux. What differentiates the flux distributions from those expected when many weakly interacting modes are involved is the large relative variation and the large skewness toward high flux: The similarity between the tails of the distributions of full simulations and those with only one toroidal mode suggests that the large events are in some sense 1D processes. In a full torus ITG simulation, there may be many toroidal modes contributing significantly to the flux, but their amplitudes are strongly correlated. This one-dimensionality is in some sense not surprising because the large events are associated with substantial modifications to 1D flux surface averaged profiles of temperature fluctuations and flows which control the mode dynamics. Given a single, normally distributed mode amplitude on each flux surface, an exponential tail naturally develops in quantities such as flux (which is proportional to the square of the mode amplitude).

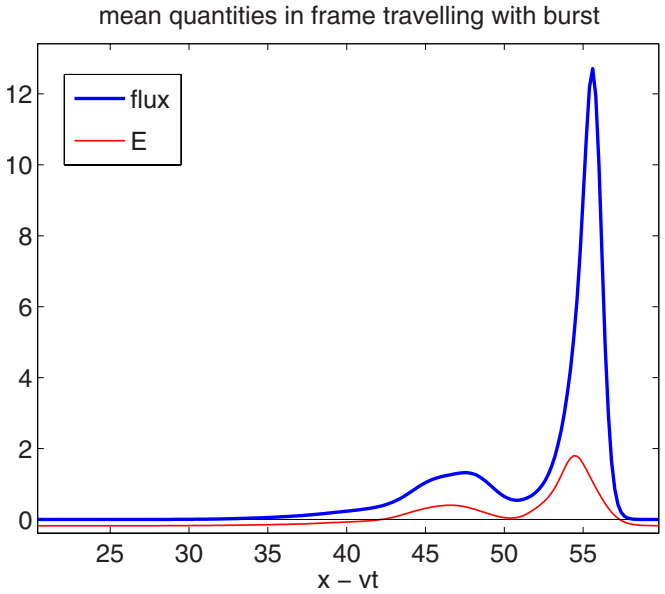


FIG. 15. (Color online) Average quantities in the burst-comoving frame in a simulation with a solitary propagating structure in the 1D model of ITG turbulence with a background shear flow $E_0'=1.1$.

Another quantity of interest is the temporal power spectrum of fluxes. We Fourier transform the flux $F(x,t)$ and examine the power spectrum $\langle F(x,\omega)^2\rangle$ averaged over the $x$ direction. This spectrum is plotted for both the 1D model and the $\rho^*=1/280$ ITG simulation in Fig. 16. The growth rate $\gamma_1$ used to normalize the frequency in the ITG simulation is taken as half the maximum linear ITG growth rate: Modes with smaller $k$ than the most rapidly growing mode dominate the transport physics in the nonlinear phase of ITG simulations due to the nonlinear downshift in mode energy, and the more effective transport for long-wavelength turbulence, and these small $k$ modes have significantly lower linear growth rates. The absolute values of the spectra here are meaningful and indicate that the relative fluctuation levels are well reproduced by the 1D simulations. There is a clear peak in the model spectrum at $\omega\sim 1$ which we identify as the inverse burst duration. The full ITG simulations appear to have similar tails at high and low frequencies and flatten at around $\omega/\gamma_1=1$, but the dependence at low frequency is not as clear because we were able to run the 1D model longer and collect better statistics. It is the low-frequency part of the spectrum below $\omega/\gamma_1=1$, which corresponds to large amplitude, long length scale events such as avalanches, which we are most interested in, rather than high frequency part of the spectrum. The fluxes in self-organized critical systems are dominated

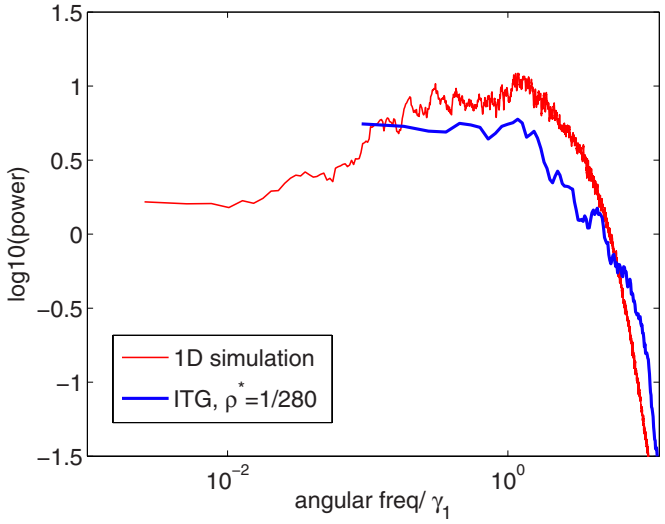


FIG. 16. (Color online) Power spectrum of flux in the 1D model compared to that in the ITG simulation with $\rho^*=1/280$.

by large low-frequency events, with the low-frequency spectra scaling like $1/f$ (although at very low frequencies the tails could be flat due to finite system size effects), but here the power spectrum of the 1D model falls off at low-frequency like $f^{0.5}$, and the power spectrum in the full ITG spectrum appears to be flat: We emphatically do not see a $1/f$ scaling in the region of interest $\omega/\gamma_1 \lesssim 1$. We would need to run the ITG simulations for an order of magnitude longer (for a thousand growth times rather than about a hundred) to convincingly test the prediction of a $f^{0.5}$ falloff at low frequency. The flattening point in the flux spectrum corresponds roughly to the (visually identified) repetition rate of small bursts at $0.7\gamma_{\mathrm{ITG}}$: Higher frequencies are expected to be associated with the behavior of the small-scale turbulent vortices. We expect to see the fingerprints of large scale structures at frequencies below $\gamma_1$, but the relative rareness of large amplitude structures is evident in the flat or downward trend in the flux spectrum.

Other quantities of interest are the relative size of quantities in the 1D model. For example, the fluctuation in shear rates due to the bursts is roughly of order of the shear in the quasistationary flows in the 1D model (both for the single bursts propagating in a constant shear flow and the fully developed turbulence): This is also the case in the ITG simulations.

Relatively frequent bursts of typical magnitude several times larger than typical flux levels propagate over scale lengths typically one or two zones wide; the intensity of typical avalanches appears to be independent of propagation extent (unlike sandpile avalanches). A propagation length of one or two zones is consistent with avalanches in previous studies of small systems which were found to cross the entire system width (Ref. 6 considers a box $100\rho_i$ in length), and with Ref. 4, which found system-length avalanches in a larger system with externally forced flows. The avalanche scaling properties indicate that the bursts are a consequence of the structure of the local turbulence, rather than the result of long-wavelength perturbations to the turbulence intensity and temperature gradient profiles.

It may be the case that in the limit of small drive, global spatial scale and time scale correlations develop typical of self-organized criticality, but the large and long gyrokinetic simulations required to demonstrate this limit have not yet been performed. The intermittent avalanchelike behavior seen in our simulations, and in Refs. 6 and 4, appears to be well described by local (i.e., flux tube) models of turbulence: We have shown that a simple 1D flux-tube model captures most of the statistical features of the bursty dynamics. This bursty process gives rise to features on the radial zonal flow wavelength scale, which is often much shorter than global length scales.

## V. SYMMETRY BREAKING BY DISPERSION IN RADIAL WAVENUMBER

The 1D model's radial inversion symmetry means that it predicts zero correlation between propagation direction and the sign of the flow shear, at odds with the simulations with Cyclone parameters. This is surprising because the 1D model includes most of the processes believed to be important for ITG turbulence, including the reaction to and forcing of zonal flows and gradient profiles. We suggested that the wave dispersion with respect to radial wavenumber might lead to burst propagation in a preferred direction: We consider adding this missing piece of physics to the 1D model equations.

The wave equations are now replaced by

$$\partial_t \tilde{n} = -i\tilde{n}E + i\tilde{\phi}(\partial_x \bar{n} - 1) + \partial_{xx}(1 + i\epsilon)\tilde{n} \tag{11}$$

and

$$\partial_t \tilde{\phi} = -i\tilde{\phi}E + i\tilde{n} + \partial_{xx}(1 + i\epsilon)\tilde{\phi}, \tag{12}$$

breaking the radial inversion symmetry. Plots of the flux as a function of radial position and time indicate that there is a favored radial propagation direction for bursts which depends on the sign of the shear (although bursts in both directions occur within any given zone).

We performed a parameter scan in $\epsilon \in [-1.5:1.5]$ for simulations with radial extent $L_x=60$ and 320 time units long. The normalized correlations between burst propagation direction and shearing rate (using the same diagnostics as for the ITG simulations), averaged over the simulation domain and $t \in [20,320]$, are plotted in Fig. 17. In this range of $\epsilon$, there is a strong, close to linear relationship between $\epsilon$ and the correlation between the shearing rate and burst propagation direction.

Using the time normalization $1/\gamma_0$ above to convert the Cyclone simulation parameters to the dimensionless units of the simulation and setting the length unit to be $1/k_\theta$ of the most unstable mode, the Cyclone dispersion relation can be written as $\omega \sim 0.5(1-k_r^2)$ ($k_\theta$ is unity in these dimensionless units), so that $\epsilon \sim 1$ for the Cyclone parameters, and a negative correlation of order of $-0.3$ is expected from our 1D model. The sign and approximate size of this correlation are consistent with our gyrokinetic results, where the correlation was around $-0.2$.

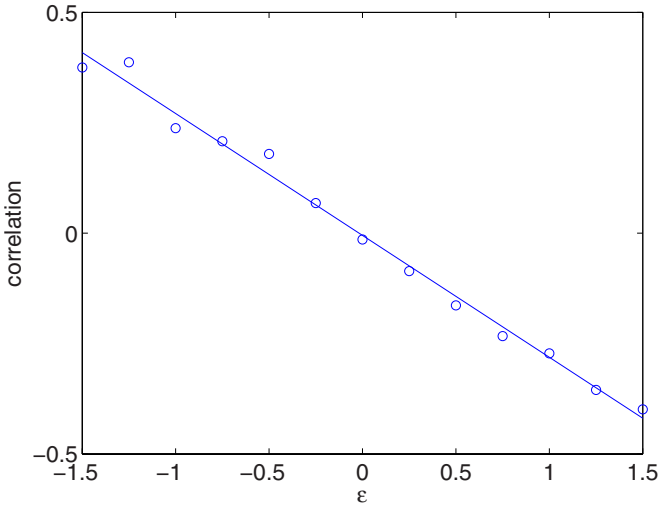


FIG. 17. (Color online) The correlation between the propagation direction of flux structures and the shearing rate (open circles) as a function of the radial dispersion coefficient $\epsilon$. A solid line shows a linear fit.

## VI. CONCLUSIONS

The bursts seen in our ITG simulations have time and length scales typical of the time and length scales of turbulent eddies, independent of global system size and characteristic amplitudes of a few times the mean flux level. The avalanches are usually localized within a shear zone, which may be considerably smaller than the system length, and their direction is correlated with the local shearing rate. These features all imply that the avalanches are local processes, rather than global relaxation events which might be dangerous for reactors.

The flux-tube-like 1D model (with only a single free parameter) we explored was able to recover many of the qualitative and quantitative features of the bursts, reproducing a similar power spectra for fluxes, similar histograms of fluxes, and qualitatively similar burst dynamics: This provides further support for our description of the avalanches as a local process. The isolated propagating bursts seen in the gyrokinetic simulations were also seen in this 1D model; stable, isolated, solitonlike structures were found numerically. The model gives a picture of the bursts in terms of nonlinear destabilization of the shear flow, a kind of subcritical turbulence analogous to that in fluid flow through a pipe. Quasilinear diffusion equations evolve fewer equations than the 1D model studied here, but are more *ad hoc*, and appear to be incapable of convincingly modeling the dynamics of the bursts of interest.

Weak-turbulence-type models would predict instantaneous flux to be a Gaussian distributed quantity, resulting from an uncorrelated sum of a large number of toroidal modes. The actual measurements from simulations indicate that there are exponential tails on the flux distribution. We explain this in terms of the dominance of zonally averaged flows which cause the amplitudes of toroidal modes to be strongly correlated: The statistics then give an exponential tail as in the case where only one toroidal mode is excited. The flux is then locally bursty, but not as bursty as, for example, in self-organized critical systems, where power-law tails are common.

There is a relationship between the sign of the shearing rate and the burst propagation direction; the sign of this relationship is consistent with a radial propagation mechanism by which sheared turbulence moves at the group velocity given by the ITG dispersion relation. The lack of a favored propagation direction for a slablike case with lower magnetic shear is also consistent with this mechanism. The magnitude of the radial dispersion gives an effect of the right size, when the radial dispersion effect is included in our 1D model. Other physics typically included in 1D turbulence models do not give a favored propagation direction for bursts. There is a strong evidence that the radial group velocity of sheared turbulence is the cause of a favored burst propagation direction.

## ACKNOWLEDGMENTS

This work was supported in part by the Swiss National Science Foundation. We acknowledge the staff of the PLEIADES2 cluster and the EPFL BlueGene supercomputer for their support. We also thank the authors of the GENE code.

[1] A. M. Dimits, G. Bateman, M. A. Beer, B. I. Cohen, W. Dorland, G. W. Hammett, C. Kim, J. E. Kinsey, M. Kotschenreuther, A. H. Kritz, L. L. Lao, J. Mandrekas, W. M. Nevins, S. E. Parker, A. J. Redd, D. E. Shumaker, R. Sydora, and J. Weiland, Phys. Plasmas **7**, 969 (2000).
[2] S. Jolliet, A. Bottino, P. Angelino, R. Hatzky, T. Tran, B. McMillan, O. Sauter, K. Appert, Y. Idomura, and L. Villard, Comput. Phys. Commun. **177**, 409 (2007).
[3] B. A. Carreras, D. Newman, V. Lynch, and P. H. Diamond, Phys. Plasmas **3**, 2903 (1996).
[4] J. Candy and R. E. Waltz, Phys. Rev. Lett. **91**, 045001 (2003).
[5] Y. Sarazin, X. Garbet, P. Grendrih, and S. Benkadda, Phys. Plasmas **7**, 1085 (2000).
[6] S. Benkadda, P. Beyer, N. Bian, C. Figarella, O. Garcia, X. Garbet, P. Ghendrih, P. Sarazin, and P. Diamond, Nucl. Fusion **41**, 995 (2001).
[7] B. McMillan, S. Jolliet, T. Tran, A. Bottino, P. Angelino, and L. Villard, Phys. Plasmas **15**, 052308 (2008).
[8] B. McMillan, S. Jolliet, T. Tran, A. Bottino, P. Angelino, and L. Villard, "Avalanche-like bursts in global gyrokinetic simulations," in 35th EPS Plasma Physics Conference, 2008.
[9] D. A. Egolf, I. V. Melnikov, and E. Bodenschatz, Phys. Rev. Lett. **80**, 3228 (1998).
[10] T. Dannert and F. Jenko, Phys. Plasmas **12**, 072309 (2005).
[11] P. Bak, C. Tang, and K. Wiesenfeld, Phys. Rev. Lett. **59**, 381 (1987).
[12] T. Hwa and M. Kardar, Phys. Rev. A **45**, 7002 (1992).
[13] A. D. Polyanin and V. F. Zaitsev, *Handbook of Nonlinear Partial Differential Equations* (Chapman and Hall, London/CRC, Boca Raton, 2004).
[14] B. N. Rogers, W. Dorland, and M. Kotschenreuther, Phys. Rev. Lett. **85**, 5336 (2000).
[15] S. Grossmann, Rev. Mod. Phys. **72**, 603 (2000).